

Electron Spin Resonance of Mn^{2+} in $\text{Eu}_2\text{M}'_3(\text{NO}_3)_{12} \cdot 24\text{H}_2\text{O}$ ($\text{M}' = \text{Zn, Co}$) Single Crystals

V. K. Jain

Department of Physics, M.D. University, Rohtak-124001, India

Reprint requests to Dr. V.K.J.; E-mail: liggavansh@yahoo.com

Z. Naturforsch. **58a**, 677 – 681 (2003); received August 25, 2003

Electron spin resonance of Mn^{2+} doped in $\text{Eu}_2\text{M}'_3(\text{NO}_3)_{12} \cdot 24\text{H}_2\text{O}$ ($\text{M}' = \text{Zn, Co}$) single crystals has been studied at 295 and 77 K using an X-band spectrometer. The observation of resolved Mn^{2+} spectra in $\text{Eu}_2\text{Co}_3(\text{NO}_3)_{12} \cdot 24\text{H}_2\text{O}$ at 295 K have been interpreted in terms of random modulation of interaction between Mn^{2+} and divalent cobalt ions by the rapid spin-lattice relaxation of cobalt ions. T_1 of divalent cobalt has been estimated to be $\sim 5 \times 10^{-12}$ s at 295 K. The superposition model is applied to the zero-field splitting parameter D . — PACS: 76.30 F

Key words: ESR; SPM; Mn^{2+} ; Co^{2+} ; Spin Lattice Relaxation.

1. Introduction

The observation of electron spin resonance (ESR) spectra of paramagnetic impurities in a paramagnetic host can be hindered by the line broadening associated with the host-impurity interaction. If host paramagnetic ions do not completely broaden the impurity ESR lines, one can study the host spin-lattice relaxation via the linewidth of the impurity ion. A system that satisfies these conditions is offered by Mn^{2+} used as impurity with cobalt constituting the paramagnetic host lattice $\text{Eu}_2\text{Co}_3(\text{NO}_3)_{12} \cdot 24\text{H}_2\text{O}$ (ECN). This is because Mn^{2+} has a long spin-lattice relaxation time, while cobalt has a very short one. Thus, despite Mn^{2+} - Co^{2+} interaction, one can observe reasonably sharp Mn^{2+} ESR spectra. Since the ESR of Mn^{2+} is easily detectable even at room temperature, many ESR investigations result in the determination of zero-field splitting (ZFS) parameters. The ZFS parameter D is quite sensitive with respect to small structural changes. The calculations of ZFS follow two approaches. In the first, which is referred to as *ab-initio* calculation, the ZFS is generally calculated using an electrostatic model of the crystal field, together with one or more of the splitting mechanisms. The second method of estimating the ZFS is by the empirical superposition model (SPM) [1]. This paper describes ESR studies of Mn^{2+} in $\text{Eu}_2\text{Zn}_3(\text{NO}_3)_{12} \cdot 24\text{H}_2\text{O}$ (EZN) and $\text{Eu}_2\text{Co}_3(\text{NO}_3)_{12} \cdot 24\text{H}_2\text{O}$ (ECN) at 295 and 77 K. The motivation is to estimate the cobalt spin-lattice relax-

ation time from Mn^{2+} linewidths. The SPM analysis of the ZFS parameter D of Mn^{2+} in EZN and ECN is also carried out.

2. Crystal Structure

The crystal structure of $\text{Eu}_2\text{Mg}_3(\text{NO}_3)_{12} \cdot 24\text{H}_2\text{O}$ (EMN), isomorphous to EZN and ECN, has been studied by Akimov et al. [2]. The primitive cell of EMN containing one formula unit is rhombohedral with lattice constants $a = 1.3116$ nm and $\alpha = 49.34^\circ$. The space group is $R\bar{3}$. The lattice parameters in hexagonal setting are $a = 1.0949$ nm, $c = 3.448$ nm. The rhombohedral unit cell contains three divalent ions situated at two different lattice sites. One occupies the C_{3i} point symmetry site (site I) and the other two occupy the C_3 point symmetry site (site II). The divalent ions are surrounded by six water molecules forming a nearly octahedral complex. Each Eu^{3+} is coordinated with twelve oxygen ions belonging to six nitrate ions, located at the corners of a somewhat irregular icosahedron.

3. Experimental

Single crystals of EZN and ECN, doped with Mn^{2+} , were grown at ~ 300 K by slow evaporation of an aqueous solution of EZN and ECN, to which 0.5 wt % Mn^{2+} was added. The crystal grows in flat hexagonal plates, the plane of which is perpendicular to the trigonal axis. The ESR experiments were performed with

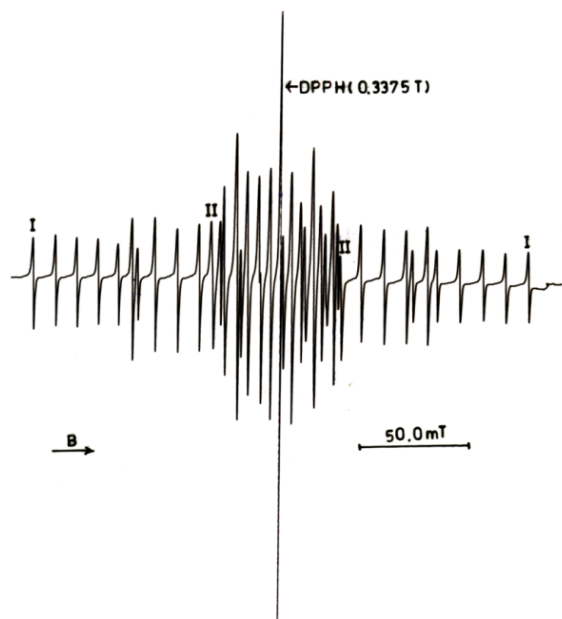


Fig. 1. The ESR spectrum of Mn^{2+} in $\text{Eu}_2\text{Zn}_3(\text{NO}_3)_{12} \cdot 24\text{H}_2\text{O}$ single crystals at 295 K. The positions of extreme hyperfine lines of Mn^{2+} complexes for two sites are designated by I and II, respectively.

a JEOL FE-3X homodyne spectrometer operating at ~ 9.45 GHz, equipped with a TE_{001} -cylindrical cavity and 100 kHz field modulation. A speck of powdered DPPH, used as a field marker (taking $g_{\text{DPPH}} = 2.0036$), was inserted simultaneously into the sample cavity. The angular variation studies were done using a JES-UCR-2X sample angular rotating device. 77 K measurements were made using a JES-UCD-2X insertion type dewar.

4. Results

For an arbitrary orientation of the crystal, the ESR spectrum consists of a number of lines corresponding to allowed and forbidden transitions. Angular variation studies of Mn^{2+} spectra reveal the presence of two inequivalent Mn^{2+} centres of unequal intensity. The Mn^{2+} substitutes for Zn^{2+} or Co^{2+} and shows the spectrum of two Mn^{2+} complexes. The spectrum having the stronger intensity is due to Mn^{2+} substituting for Zn^{2+} (Co^{2+}) at site II while the spectrum having the lower intensity is due to Mn^{2+} at site I (Fig. 1). The Mn^{2+} centre occupying the site II is more intense because there are twice as many II sites than I sites. It was found that the principal z -axes of two Mn^{2+}

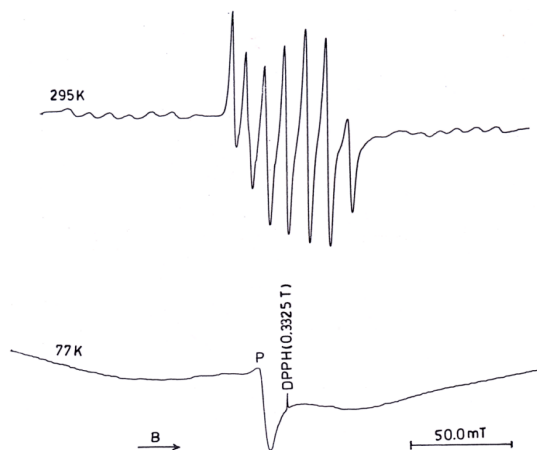


Fig. 2. The ESR spectrum of Mn^{2+} in $\text{Eu}_2\text{Co}_3(\text{NO}_3)_{12} \cdot 24\text{H}_2\text{O}$ single crystals at 295 K and 77 K with B parallel to the z -axis. The line marked P is due to an impurity in the cavity.

complexes are along the trigonal axis (c -axis) and x -axes perpendicular to the c -axis. The spectra of Mn^{2+} showing a large ZFS (site I) were measured for various angles of the magnetic field relative to c -axis. A $\pi/3$ rotational symmetry of the spectrum was observed when the crystal was rotated about the trigonal axis. Detailed angular variation studies could not be made for ECN because of large linewidths. The ESR spectrum of Mn^{2+} in ECN with the z -axis parallel to the magnetic field is shown in Figure 2.

The intense lines at the centre of the spectrum at 295 K belong to Mn^{2+} at site II. Magnetic field measurements have been made for the Mn^{2+} complex in ECN having a large ZFS (site I). For site I also, except for $M = \pm 5/2 \leftrightarrow \pm 3/2$, the lines in the spectrum are practically unobservable as the linewidths of various transitions increase as one goes from outer to inner transitions. The linewidth of Mn^{2+} in ECN at ~ 295 K is ~ 4.0 mT for $M = \pm 3/2 \leftrightarrow \pm 5/2$, while for EZN it is ~ 1.0 mT. Because of the magnitude of the ZFS and the large linewidths, the two hyperfine lines of the $M = \pm 3/2 \leftrightarrow \pm 1/2$ transitions overlap with the two hyperfine lines of the $M = \pm 5/2 \leftrightarrow \pm 3/2$ transitions, resulting in the appearance of more than six lines for the outer transitions.

However in EZN, where the magnitude of the ZFS is nearly the same as that of ECN and the linewidths are small, the ESR lines of various transitions are well resolved. Further, in EZN the first hyperfine line of the $M = -1/2 \rightarrow -3/2$ transition appears before the last

hyperfine line of the $M = -3/2 \rightarrow -5/2$ transition, and the last hyperfine line of the $M = +3/2 \rightarrow +1/2$ transition, appears after the first hyperfine line of the $M = +5/2 \rightarrow +3/2$ transition. Experiments were also performed at 77 K to study the effect of paramagnetic Eu^{3+} and Co^{2+} ions on the Mn^{2+} spectra. In EZN at 77 K, except for an increase in the spread of the spectrum, no changes in the g -values or in the linewidths are observed. This indicates that Eu^{3+} behaves like a diamagnetic ion down to 77 K. However, in ECN it was found that at 77 K the width of the resonance lines increases, and only a broadened spectrum is observed (Fig. 2). On raising the temperature again, the well resolved spectrum reappears, indicating that the smearing out of the spectrum at low temperature is due to increased linewidths on lowering the temperature.

5. Discussion

The ESR spectrum of Mn^{2+} for both sites can be described by a spin-Hamiltonian of the form [3]

$$H = \beta_e \mathbf{S} \cdot \mathbf{g} \cdot \mathbf{B} + D [S_z^2 - (35/12)] - (7/36)(a - F) [S_z^4 - (95/14)S_z^2 + (81/16)] + (a\sqrt{2}/36) \{ S_+ [S_+^3 \exp(-3i\varphi) + S_-^3 \exp(3i\varphi)] + [S_+^3 \exp(-3i\varphi) + S_-^3 \exp(3i\varphi)] S_z \} + \mathbf{S} \cdot \mathbf{A} \cdot \mathbf{I},$$

where the z -axis is parallel to the trigonal axis of the crystal. The symbols have their usual meaning, and $S = I = 5/2$ for $^{55}\text{Mn}^{2+}$. The best-fit parameters for the 295 and 77 K Mn^{2+} ESR spectra are listed in Table 1. The signs of the parameters (given in Table 1) are only relative. The relative signs of the parameters D and A_{\parallel} (A_z) are obtained by comparing the second-order shifts in the separation between hyperfine components for the various electronic transitions [4]. The sign of D is then obtained by assuming A_{\parallel} to be negative, as in all the materials where the signs have been determined A_{\parallel} has been found to be negative [5]. From Table 1 it is clear that the ZFS parameter D is very different for the two sites and is temperature sensitive. The different values of D for Mn^{2+} at two sites indicate that the two sites differ greatly in the crystal field seen by the ions.

Assuming the ZFS to be solely due to the distortion of the first coordinate sphere of the oxygens of the water molecules, the experimental ZFS can be compared with those calculated from the crystal structure data for the pure host compound. The SPM allows such a comparison [1]. The SPM is based on two assumptions:

Table 1. Spin-Hamiltonian parameters for Mn^{2+} in $\text{Eu}_2\text{M}''_3(\text{NO}_3)_{12} \cdot 24\text{H}_2\text{O}$ ($\text{M}'' = \text{Zn, Co}$) single crystals. All crystal field and hyperfine parameters are in units of 10^{-4} cm^{-1} .

Spin-Hamiltonian Parameters	$\text{M}'' = \text{Zn}$				$\text{M}'' = \text{Co}$
	Site I		Site II		Site I
	295 K	77 K	295 K	77 K	295 K
D	-193(2)	-223(2)	12(2)	-72(2)	-191(3)
$a - F$	-4(1)	-6(1)	6(2)	8(2)	-8(2)
g_{\parallel}	2.004(2)	2.003(2)	2.006(2)	2.008(3)	1.994(3)
g_{\perp}	2.003(2)	2.003(2)	2.005(2)	2.005(3)	1.997(3)
A_{\parallel}	-90(1)	-90(1)	-88(2)	-88(2)	-90(2)
A_{\perp}	-90(1)	-90(1)	-88(2)	-89(2)	-90(2)

(i) ZFS is due to the close neighbour ions and (ii) ZFS is given by the sum of axially symmetric contributions of the i ligands of the MX_i unit. The contributions of more distant neighbours, as well as the interaction between the ligands are ignored. The ZFS parameter D is written as

$$b_2^0 = D = \sum K_2^0(\theta_i, \varphi_i) \bar{b}_2(R_i),$$

where $K_2^0 = (1/2)(3 \cos^2 \theta - 1)$, the summation runs over all ligands. R_i, θ_i, φ_i are the spherical coordinates of the i -th ligand (the paramagnetic ion is placed at the origin). $\bar{b}_2(R_i)$ is a scalar quantity, called the second-order intrinsic ZFS parameter. It depends characteristically on the specific metal-ligand combination [6]. In the SPM framework it is assumed [1] that the change of $\bar{b}_2(R_i)$ on going from a reference distance R_0 to another R_i is given by the empirical power law [6]

$$\bar{b}_2(R_i) = \bar{b}_2(R_0)(R_0/R_i)^{t_2},$$

where the power law exponent t_2 is 7 ± 1 for Mn^{2+} . $R_0 = 0.22 \text{ nm}$ is the reference distance of Mn^{2+} surrounded by six oxygens [6]. $\bar{b}_2(R_0) = -0.05 \text{ cm}^{-1}$ [6] is used. This value is obtained experimentally from the analysis of the spin-Hamiltonian parameter D corresponding to Mn^{2+} placed in different lattices, all of which have the same ligand (oxygen or water) and the same coordination number 6 [6].

The value of the ZFS parameter D of Mn^{2+} in EZN and ECN indicates that the whatever the difference between the structure of EZN and ECN as regards to the lattice parameters and coordinates of the ions, the substitution of Mn^{2+} in place of a divalent cation forms $[\text{Mn}(\text{H}_2\text{O})_6]^{2+}$ complexes which have nearly the same configuration irrespective of the host. The crystal structure of ECN and EZN has not been determined. However, it is expected that bond lengths of Co^{2+} - H_2O and Zn^{2+} - H_2O in ECN and EZN would be larger

than Mg^{2+} - H_2O in EMN, as the ionic radii of Mg^{2+} , Co^{2+} and Zn^{2+} are 0.066, 0.072 and 0.074 nm [7], respectively. In the SPM analysis the structural data of EMN are used. Mg^{2+} in EMN at site I is surrounded by six water molecules at a distance $R = 0.2051$ nm, and at site II is surrounded by two sets of three water molecules, each as nearest neighbours at distances 0.2051 nm and 0.2059 nm. The angle θ that Mg-O makes with the c axis at site I is 54.52° , and for site II the angles are 54.36° and 123.12° . The calculated values of the ZFS parameter D are $-26(2) \times 10^{-4} \text{ cm}^{-1}$ and $102(2) \times 10^{-4} \text{ cm}^{-1}$ for site I and II, respectively. The SPM predicts the correct sign for both sites. The calculated value of D for site I is smaller than the experimental value and larger for site II.

In these calculations the assumption has been made that the crystalline structure in the vicinity of the magnetic ion equals that of the host lattice. The difference in the calculated and experimental values of D may be in principle result from the local relaxation. It has been shown that, if R (metal-ligand bond distance) $>$ normal Mn-ligand bond distance, the introduction of substitutional Mn^{2+} gives rise to an inward relaxation, while the opposite occurs for $R <$ Mn-ligand bond distance [8]. The ionic radius of Mn^{2+} is 0.080 nm [7]. Therefore, Mn^{2+} substitution for Co^{2+} or Zn^{2+} would allow some expansion of the O^{2-} octahedron around manganese. A movement of oxygen along the c axis is assumed such that the Mn-oxygen bond length increases from that Mg(Co,Zn)-oxygen. This causes a change in the value of θ . It is found that an increase of about 2% in bond lengths (from 0.2051 to 0.2094 nm) causes the angle θ to change to 52.92° for site I. An increase of about 0.78% in bond length for site II causes θ to change to 53.77° and 123.84° . These values of R and θ lead to D values $-192 \times 10^{-4} \text{ cm}^{-1}$ and $25 \times 10^{-4} \text{ cm}^{-1}$ for sites I and II, respectively. A change of bond lengths of about 3%–4% is observed from EXAFS measurements in $KZnF_3$ and $KCdF_3$ doped with Mn^{2+} [8].

The observation of well resolved ESR spectra of Mn^{2+} impurity ions in paramagnetic ECN at high temperature is contrary to the expectation that the impurity resonance lines should be broadened due to spin-spin interaction between the host and paramagnetic ions. The observed line widths of Mn^{2+} in ECN can be understood on the basis of host spin-lattice relaxation narrowing. Mitsuma [9] proposed that the fast spin-lattice

relaxation of the host can randomly modulate the dipolar and exchange interaction between the paramagnetic host and impurity ions, resulting in what is called "host spin-lattice relaxation narrowing".

The cobalt ions are fast relaxing ions because their orbital angular momentum is not quenched, so these ions are expected to show narrowing effects. It has been shown that the requirements stated in motional narrowing theory [9, 10] can be met in the case of divalent manganese in cobalt salts [10, 11] at ~ 295 K and ~ 9.5 GHz. It can be shown that the requirements stated in motional narrowing theory can also be met in the case of Mn^{2+} doped ECN. Thus the observation of resolved ESR spectra of Mn^{2+} in ECN and its broadening on lowering the temperature can be attributed to the host spin-lattice relaxation narrowing.

The impurity ion linewidths provide information about the host T_1 when the host spin-lattice relaxation narrowing mechanism is effective. According to the approach used by Saraswat and Upreti [10] for Mn^{2+} doped cobalt compounds, one can estimate T_1 from the formula [11]

$$T_1 = 3h\Delta B_{\text{imp}}/20g_{\text{host}}\beta_e B_d^2,$$

where $B_d^2 = 5.1(g_{\text{host}}\beta_e n)^2 S_h(S_h + 1)$, ΔB_{imp} is the impurity linewidth, B_d the linewidth due to dipole-dipole interaction, β_e the Bohr magneton, S_h is the host effective spin and n the number of paramagnetic spins (Co^{2+}) per unit volume that can be calculated from the crystallographic data. It is found that T_1 of cobalt at ~ 295 K is $\sim 5 \times 10^{-12}$ s. In the calculations the crystallographic data of EMN have been used, and n is found to be 2.5×10^{27} spins/ m^3 . The value of $g_h = 7.35$ is taken from $La_2Mg_3(NO_3)_{12} \cdot 24H_2O : Co^{2+}$ data [12]. S_h is the effective spin and is equal to $1/2$. It is observed that the Mn^{2+} linewidths in isomorphous EZN (which is mainly due to dipolar interaction among Mn^{2+} spins) are independent of temperature down to 77 K. Therefore, in the calculations of T_1 of cobalt, ΔB_{imp} is taken as the difference between the measured ESR linewidth of Mn^{2+} in ECN and EZN when B is parallel to the z -axis. The order of T_1 for Co^{2+} is found to be quite satisfactory since extrapolation to 300 K the data of Zevere and Petelina. [13] for two cobalt sites in Al_2O_3 give $T_1 = 3 \times 10^{-11}$ s, and 3×10^{-12} s, and the data of Pryce [14] for Co^{2+} in MgO give $T_1 = 10^{-11}$ s.

- [1] D.J. Newman and W. Urban, *Adv. Phys.* **24**, 793 (1975); D.J. Newman and B. Ng., *Rep. Progr. Phys.* **52**, 699 (1989).
- [2] V.M. Akimov, A.I. Yanovskii, Yu. T. Struckov, A. K. Molodkin, Yu. A. Grigorev, and N. K. Novikov, *Russ. J. Inorg. Chem.* **32**, 92 (1987).
- [3] S. Geschwind, *Phys. Rev.* **121**, 363 (1961).
- [4] W. Low, *Paramagnetic Resonance In Solids (Solid State Physics, Suppl. 2)* Academic Press, New York 1960, p. 71.
- [5] A. Abragam and B. Bleaney, *Electron Paramagnetic Resonance of Transition Ions*, Clarendon Press, Oxford 1970, p. 439.
- [6] M. Hemming and G. Lehmann in "Electronic Magnetic Resonance of the Solid State", J. A. Weil (Ed.) Canadian Society for Chemistry, Ottawa 1987, p. 163.
- [7] *CRC Handbook of Chemistry and Physics*, D. R. Lide (Ed.) 1990/91, p. 12-1.
- [8] M. T. Barriuso and M. Moreno, *Phys. Rev. B* **29**, 3623 (1984).
- [9] T. Mitsuma, *J. Phys. Soc. Japan* **17**, 128 (1962).
- [10] G. C. Upreti and R. S. Saraswat, *Magn. Reson. Rev.* **7**, 215 (1982).
- [11] M. R. St. John, Ph. D. Thesis, University of California, Berkeley 1975, unpublished.
- [12] J. W. Culvahouse and D. P. Schink, *Phys. Rev.* **187**, 671(1969).
- [13] G. M. Zverev and N. G. Petelina, *Sov. Phys. JETP* **15**, 820 (1962).
- [14] M. H. L. Pryce, *Proc. Roy. Soc. London A* **283**, 433 (1965).